A model predictive wind farm controller with linear parameter-varying models

Boersma, Sjoerd; Rostampour, Vahab; Doekemeijer, Bart; van Wingerden, Jan-Willem; Keviczky, Tamás

DOI
10.1016/j.ifacol.2018.11.020

Publication date
2018

Document Version
Final published version

Published in
IFAC-PapersOnLine

Citation (APA)
Boersma, S., Rostampour, V., Doekemeijer, B., van Wingerden, J.-W., & Keviczky, T. (2018). A model predictive wind farm controller with linear parameter-varying models. *IFAC-PapersOnLine*, *51*(20), 241-246. https://doi.org/10.1016/j.ifacol.2018.11.020

Available online at www.sciencedirect.com

ScienceDirect

IFAC Papers Online CONFERENCE PAPER ARCHIVE

IFAC PapersOnLine 51-20 (2018) 241–246

A Model Predictive Wind Farm Controller with Linear Parameter-Varying Models

Sjoerd Boersma, Vahab Rostampour ⋆ , Bart Doekemeijer Jan-Willem van Wingerden and Tamás Keviczky ⋆

Delft Center of Systems and Control, Delft University of Technology, The Netherlands. (e-mail: {v.rostampour, s.boersma, j.w.vanwingerden, t.keviczky}@tudelft.nl)

Abstract: In this paper, we present an implementation of a model predictive controller (MPC) for wind farm power tracking problem. The controller is evaluated in the high-fidelity PArallelized Large-eddy simulation Model (PALM). By taking measurements from PALM, we show that the closed-loop MPC can provide power reference tracking while reducing force variations on a farm level by solving a constrained optimization problem at each time step. A six turbine wind farm case study is presented in which the controller operates with yawed turbines that increases the potential power that can be harvested with the wind farm, and we show that it is possible to track a reference power signal that temporarily exceeds the power harvested when operating under the so-called greedy control settings.

Keywords: Wind farm, Model Predictive Control, Large-eddy simulations

1. INTRODUCTION

A large part of all renewable energy finds its origin in wind (Enerdata, 2017). Consequently, the stimulation of wind power penetration in the network becomes more important. This can be stimulated by the provision of grid facilities such as secondary frequency regulation by wind farms. Here, the objective is to track a power reference signal with a wind farm by dynamically de- and uprating the turbines. Investigating and understanding the problem should result in a smoother penetration of wind energy in the energy market.

In this paper the objective is to have the total wind farm's power generation output track a certain demanded power signal generated by operators, during a time span of several minutes (Ela et al., 2014). In wind farms, this objective could be separated into two tasks: 1) distribution of the wind farm power reference signal to reference signals for the individual turbines in the farm and 2) tracking of the local references by the individual turbines. In (Shapiro et al., 2017), both these tasks are solved in a centralized wind farm controller, which solves a constrained optimization problem containing wake and turbine models. In (van Wingerden et al., 2017; Vali et al., 2018), no wake model or constraints have been taken into account in the controller providing tracking. Wind farm controllers that provide power tracking are also presented in (Spudić et al., 2010; Madjidian et al., 2011; Biegel et al., 2013; Siniscalchi-Minna et al., 2018). Although interesting, these controllers are not tested in a high-fidelity simulation environment, which makes it difficult to assess if the therein presented results can be obtained in practice. This work is focussed on controller development in a high-fidelity simulation environment and consequently is focussed on the flow dynamics in a wind farm.

This paper proposes a reference tracking framework in which a model predictive controller (MPC) solves a constrained optimization problem containing a simplified wind farm model that is updated each time step according to local rotor-averaged wind speed measurements. The applied reference signal distribution is based on the yet to be defined available power. This results in good tracking performance for reference signals below the averaged power harvested with greedy control settings, i.e., the time-averaged power harvested with maximal control settings. However, reference signals above this limit will not be satisfactorily tracked. Therefore, the steady-state wind farm model as presented in (Bastankhah and Porte-Agél, 2016) is employed to find the optimal steady-state yaw angles. The MPC is then tested with optimal steady-state yaw angles and we show that our proposed framework can track reference signals even above the greedy limit. The proposed MPC is tested in the high-fidelity PArallelized Large-eddy simulation Model (PALM) considering a six turbine wind farm case study. An important contribution of this paper is to provide the reader with additional simulation results compared to (Boersma et al., 2018).

2. WIND FARM SIMULATION MODEL

The PArallelized Large-eddy simulation Model (PALM) is a high-fidelity wind farm model (Maronga et al., 2015). The PALM model is based on the filtered incompressible Navier-Stokes equations. It includes the actuator disk model (ADM) (Betz, 1926) to determine the turbine's forcing terms acting on the flow. This turbine model is

⋆ These authors were supported by the Uncertainty Reduction in Smart Energy Systems (URSES) research program funded by the Dutch organization for scientific research (NWO) and Shell under the project Aquifer Thermal Energy Storage Smart Grids (ATES-SG) with grant number 408-13-030.

2405-8963 © 2018, IFAC (International Federation of Automatic Control) Hosting by Elsevier Ltd. All rights reserved.
Peer review under responsibility of International Federation of Automatic Control.
10.1016/j.ifacol.2018.11.020

efficient due its lower requirements of grid resolution and coarser allowed time-stepping as compared to having to resolve detailed flow surrounding rotating blades (Meyers and Meneveau, 2010). A consequence of choosing the ADM is that the control signals are the disk-based thrust coefficient $C'_{T_i}(t)$ following (Meyers and Meneveau, 2010). Simulations are initialized as follows: a fully developed flow field is generated in the precursor with U_∞=8 [m/s] and V_∞=W_∞=0 [m/s] and a TI_∞ of approximately 6% at hub-height in front of the wind farm. Then, for the specific topology considered in this work, the flow is propagated 900 seconds in advance with constant control settings so that the wakes are fully developed. Here, non-cyclic boundary conditions and time-dependent turbulent inflow data are imposed by using a turbulence recycling method (Maronga et al., 2015). The flow field obtained after these 900 seconds is utilized as initial flow field for the simulation results presented in this paper. We assume that the measured variables at time t are 1) the force that a turbine exerts on the flow $F_i(t)$, 2) the power generated by a turbine $P_i(t)$ and 3) the rotor-averaged wind velocity $v_i(t)$ for $i = 1, 2, \ldots, \aleph$ with $\aleph$ the number of turbines in the farm.

3. CONTROLLER MODEL

The MPC paradigm applies the receding horizon principle in which a finite-time constrained optimization problem is solved at each time step using future predictions of the system's state. This highlights the necessity of having a representative dynamical model to predict state trajectories of the real system. However, due to nonlinear dynamics and uncertain atmospheric conditions, it is challenging to obtain a dynamical wind farm model suitable for online control (Boersma et al., 2017). In this paper we therefore employ wind turbine models with varying dynamical system parameters, since the measured rotor-averaged wind velocity is a time-varying parameter. This avoids the challenge of including a wake model in the optimization problem.

Consider now the turbine models employed in the MPC for $i = 1, 2, \ldots, \aleph$ that are based on a filtered version of the actuator disk theory as follows:

$$P_i(t) = \frac{\pi D^2}{8}\Big(v_i(t)\cos[\gamma_i(t)]\Big)^3 \hat{C}'_{T_i}(t)\,, \tag{1a}$$

$$F_i(t) = \frac{\pi D^2}{8}\Big(v_i(t)\cos[\gamma_i(t)]\Big)^2 \hat{C}'_{T_i}(t)\,, \tag{1b}$$

$$C'_{T_i}(t) = \tau\frac{\mathrm{d}\hat{C}'_{T_i}(t)}{\mathrm{d}t} + \hat{C}'_{T_i}(t)\,, \tag{1c}$$

where $P_i(t)$ is the filtered generated power, $F_i(t)$ the filtered force, $C'_{T_i}(t)$ the control signal, $\hat{C}'_{T_i}(t)$ the first-order filtered control signal, γ_i the yaw angle, and $v_i(t)$ the rotor-averaged longitudinal wind velocity. The parameters $\tau \in \mathbb{R}^+$ is the filter's time constants that acts on the control signal. Temporally discretizing (1c) using the zero-order hold method with sample period $h = 1$ [s] and lifting the state variables of the turbines results in the following state-space linear parameter-varying system model:

$$\boldsymbol{x}_{k+1} = A\boldsymbol{x}_k + B(\boldsymbol{v}_k, \boldsymbol{\gamma}_k)\boldsymbol{C'_{T,k}}, \quad \boldsymbol{y}_k = \boldsymbol{x}_k, \tag{2}$$

where $x_k = [x_{1,k}\ x_{2,k}\ \cdots\ x_{\aleph,k}] \in \mathbb{R}^{3\aleph}$ such that $x_{i,k} = \begin{bmatrix} F_{i,k} & P_{i,k} & \hat{C}'_{T_{i,k}} \end{bmatrix} \in \mathbb{R}^3$, and $\boldsymbol{C'_{T,k}}, \boldsymbol{\hat{C}'_{T,k}} \in \mathbb{R}^{\aleph}$. The system matrices are defined as follows:

$$A = \texttt{blkdiag}\Big(A_1, A_2, \ldots, A_\aleph\Big)\,,$$

$$B(\boldsymbol{v}_k) = \texttt{blkdiag}\Big(B_1(v_{1,k}), B_2(v_{2,k}), \ldots, B_\aleph(v_{\aleph,k})\Big)\,,$$

where $\texttt{blkdiag}(\cdot)$ denotes block diagonal concatenation of matrices or vectors $A_i \in \mathbb{R}^{3\times3}$ and $B_i(v_{i,k}) \in \mathbb{R}^{3\times1}$, respectively, for $i = 1, 2, \ldots, \aleph$.

4. CONTROL STRATEGY

4.1 Reference distribution

Based on (Hansen et al., 2006), we consider the following reference distribution:

$$P^{\mathrm{ref}}_{i,k} = \min\left(\frac{P^{\mathrm{ref}}_k}{\sum_{i=1}^{\aleph} P^{\mathrm{aiv}}_{i,k}} P^{\mathrm{aiv}}_{i,k}\ ,\ P^{\mathrm{aiv}}_{i,k}\right), \tag{3a}$$

$$P^{\mathrm{aiv}}_{i,k} = \frac{\pi D^2}{8}[v_{i,k}\cos(\gamma_i)]^3 C'_{T,\max}\,, \tag{3b}$$

where $P^{\mathrm{aiv}}_{i,k}$ the available power for the i^{th} turbine, P^{ref}_k the wind farm power reference signal, $P^{\mathrm{ref}}_{i,k}$ the reference signal for the i^{th} turbine, and $C'_{T,\max} = 2$ the maximum value of the control signals.

4.2 Model Predictive Controller

Consider the cost function of the MPC at each time step k to be as follows:

$$\begin{aligned} V(\boldsymbol{x}_k, \boldsymbol{x}^{\mathrm{ref}}_{k_0}, \boldsymbol{C'_{T,k}}) :=& (\boldsymbol{x}_k - \boldsymbol{x}^{\mathrm{ref}}_{k_0})^T Q(\boldsymbol{x}_k - \boldsymbol{x}^{\mathrm{ref}}_{k_0}) \\ &+ (\boldsymbol{x}_k - \boldsymbol{x}_{k-1})^T S(\boldsymbol{x}_k - \boldsymbol{x}_{k-1}) \\ &+ \boldsymbol{C'_{T,k}}^T R\, \boldsymbol{C'_{T,k}}, \end{aligned}$$

where $Q, S \in \mathbb{R}^{3\aleph\times3\aleph}$, and $R = I_\aleph \cdot r \in \mathbb{R}^{\aleph\times\aleph}$ are weighting coefficient matrices. Q and S are defined to be:

$$Q = I_\aleph \otimes \begin{pmatrix} 0 & 0 & 0 \\ 0 & q & 0 \\ 0 & 0 & 0 \end{pmatrix}, S = I_\aleph \otimes \begin{pmatrix} s & 0 & 0 \\ 0 & 0 & 0 \\ 0 & 0 & 0 \end{pmatrix}, \tag{4}$$

where $\otimes$ is the Kronecker product and $r, q, s \in \mathbb{R}$ are controller tuning variables such that by tuning each weight one can increase or decrease the importance of the corresponding term in the cost function. The variable $\boldsymbol{x}^{\mathrm{ref}}_{k_0}$ in the cost function represents the reference tracking signal and it is considered to be

$$\boldsymbol{x}^{\mathrm{ref}}_{k_0} = \begin{pmatrix} 0 & P^{\mathrm{ref}}_{1,k_0} & 0 & 0 & P^{\mathrm{ref}}_{2,k_0} & 0 & \ldots & 0 & P^{\mathrm{ref}}_{\aleph,k_0} & 0 \end{pmatrix}^T \in \mathbb{R}^{3\aleph}.$$

Now we are in a position to formulate a finite-time constrained optimization problem at time step k_0 for the complete wind farm as:

$$\min_{\{\boldsymbol{C'_{T,k}}\}_{k=k_0}^{k_0+N_h}} \quad \sum_{k=k_0}^{k_0+N_h} V(\boldsymbol{x}_k, \boldsymbol{x}^{\mathrm{ref}}_{k_0}, \boldsymbol{C'_{T,k}}) \tag{5a}$$

subject to (5b)

$$\boldsymbol{x}_{k+1} = A\boldsymbol{x}_k + B_u(\boldsymbol{v}_{k_0}, \boldsymbol{\gamma}_{k_0})\boldsymbol{C'_{T,k}} + B_r P^{\mathrm{ref}}_k, \tag{5c}$$

$$C'_{T,\min} \le C'_{T_i,k} \le C'_{T,\max}, \quad |C'_{T_i,k} - C'_{T_i,k\text{-}1}| < \mathrm{d}C'_T,$$

where $C'_{T,\max} = 2$, $C'_{T,\min} = 0.1$, and $\mathrm{d}C'_T = 0.2$ represent the maximum and minimum bounds on the control variables and its variation, respectively, whereas x_{k_0} and v_{k_0} denote the measured state and rotor-averaged wind velocity at time k_0, respectively. Note that the optimization problem is formulated on a farm level, although the optimization problems could also be solved locally. However, this work is a step in the direction of a centralized wind farm MPC without reference distribution, and hence we employ this formulation.

5. SIMULATION RESULTS

The PALM simulation results are all of a neutral atmospheric boundary layer and will be discussed in this section. We first present a simulation study in which the controller is working under yawed conditions that, as will be shown, increases the set of trackable wind farm reference signals. We then study the effect of the controller on the variation of the axial force and finally, we provide a simulation study where the controller is tested under time-varying atmospheric conditions. More precisely, during the 900 second simulation time, the lateral flow velocity component is perturbed.

In all the aforementioned case studies the controller is applied to a wind farm with specifications as described in (Boersma et al., 2018). We note that in the six turbine case study presented in this work, the controller takes approximately 0.07 [s] on a regular notebook and single core for evaluating new control signals. The CPLEX solver is used to solve the optimization problem.

5.1 Simulation Performance Measures

In order to assess the controller performance under different settings, two criteria are introduced

$$\gimel = \left(\frac{||P_k^{\mathrm{ref}} - \sum_{i=1}^{\aleph} P_{i,k}||_2}{e_{\mathrm{base}}} - 1 \right) \cdot 100\ \%\,, \qquad (6a)$$

$$\mathrm{d}F_i = \left(\frac{\sum_{k=1}^{N} (F_{i,k} - F_{i,k-1})^2}{dF_{i,\mathrm{base}}} - 1 \right) \cdot 100\ \%\,, \qquad (6b)$$

with $dF_{i,\mathrm{base}} = \sum_{k=1}^{N} (F_{i,k} - F_{i,k-1})^2$ and $e_{\mathrm{base}} = ||P_k^{\mathrm{ref}} - \sum_{i=1}^{\aleph} P_{i,k}||_2$ for $s = 0$. Note that a negative $\gimel$ indicates improved tracking and a negative $\mathrm{d}F_i$ indicates decreased force variations over the complete simulation time with respect to the $s = 0$ case.

5.2 Optimal Yaw Actuation Setting

The proposed MPC is evaluated under zero yaw and yaw settings for maximal power capture in steady-state with the prediction horizon $N_h = 15$ that is found after tuning the controller. The wind farm power reference signal is defined as:

$$P_k^{\mathrm{ref}} = 0.8 P^{\mathrm{greedy}} + 0.3 P^{\mathrm{greedy}} \delta P_k\,, \qquad (7)$$

where δP_k is a normalized "RegD" type AGC signal (Pilong, 2013) coming from an operator, and $P^{\mathrm{greedy}} \approx 7.5$ [MW] presents the time-averaged produced wind farm power under greedy control, i.e., with $C_{Ti,k} = 2$ and $\gamma_i = 0$. Note that, for a short period, more power is demanded from the farm than the power harvested under greedy control. The simulation results are obtained with controller parameters $N_h = 15, q = 10^4, r = 10^4, s = 0$ that are found after tuning and are presented in Fig. 1. The top plot in Fig. 1 illustrates that the power reference cannot be tracked without an undesired error for a period between 300 and 600 seconds. This is due to a demanded power larger than the previously defined available power in the farm under the imposed reference distribution (see (3)). The authors in (Fleming et al., 2016) illustrated that redirecting the wake can be beneficial during active power control when demanding more power from the farm than available under non-yawed turbines. Following this idea, optimal steady-state yaw settings are imposed during the complete simulation. These settings, $\gamma_i = \gamma_i^* = \{-24.3, -24.3, -16.2, -16.2, 0, 0\}$ [deg], are found using the wind farm optimization tool FLORIS (Doekemeijer, 2018) in which a steady-state wind farm model (Bastankhah and Porte-Agél, 2016) is employed to predict and maximize the steady-state power production for different yaw settings. The bottom plot of Fig. 1 illustrates that better tracking is ensured when the turbines are set to their optimal yaw settings with respect to the case when $\gamma_i = 0$. This is due to the increase of available power when controlling under optimal yaw settings and consequently, reference signals with higher amplitudes can be tracked. Instead of yawing the turbines, it could also be possible to increase the available power by imposing a different distribution than presented in (1a). This idea is however not further investigated in this work. The tracking results of the individual turbines in the nonyawed case can be found in Fig. 2 and the control signals of the yawed case in Fig. 3.

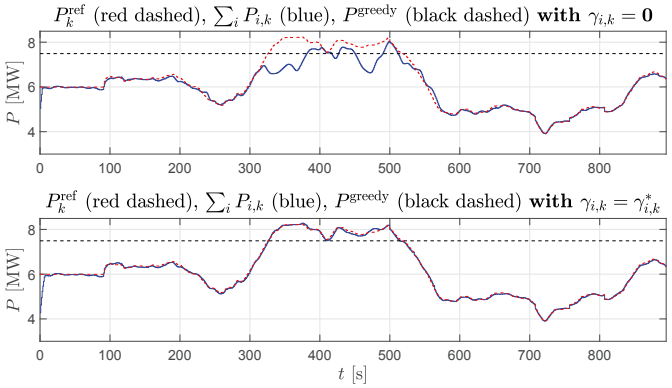

Fig. 1. Wind farm tracking results of the controller under different yaw settings.

5.3 Minimizing Axial Force Variation

We now study the effect of the controller tuning parameter s (see (5)). This weight acts on the axial force variation and an increasing s makes the optimization penalizes the variation more. One could consider this variation as a measure for turbine fatigue and it is therefore interesting to minimize this quantity, possibly expanding the turbine's lifetime. The following wind farm power reference signal is applied:

$$P_k^{\mathrm{ref}} = 0.7 P^{\mathrm{greedy}} + 0.2 P^{\mathrm{greedy}} \delta P_k\,. \qquad (8)$$

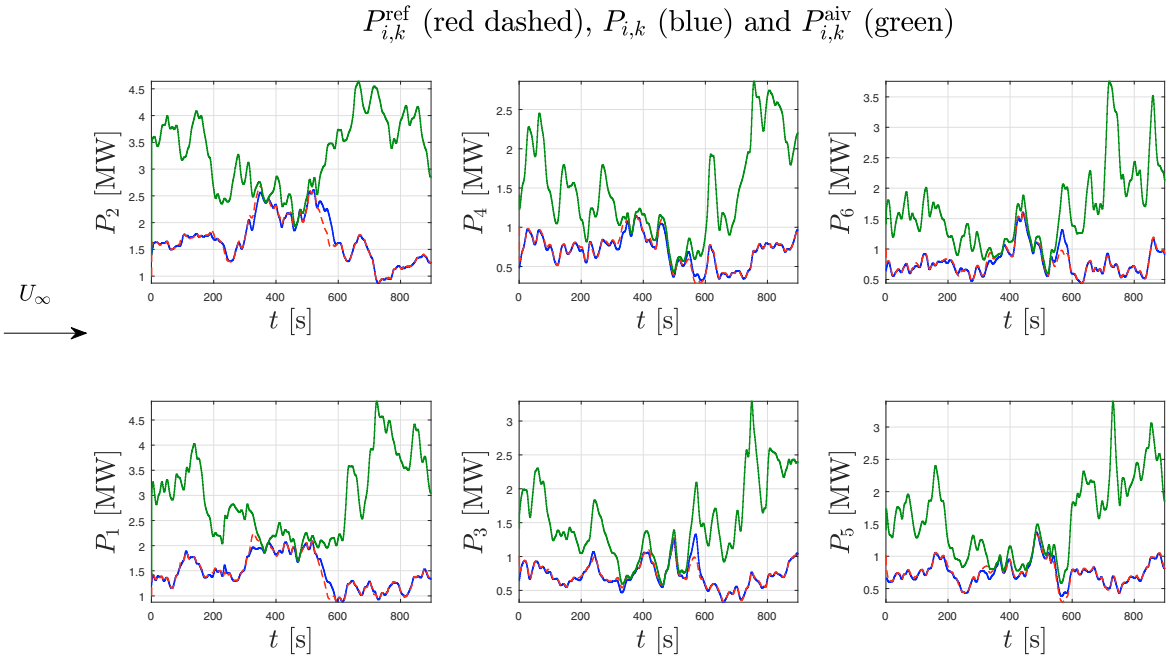

Fig. 2. Turbine tracking results of the controller under $\gamma_i = 0$. The black arrow on the left of the figure indicates the wind direction.

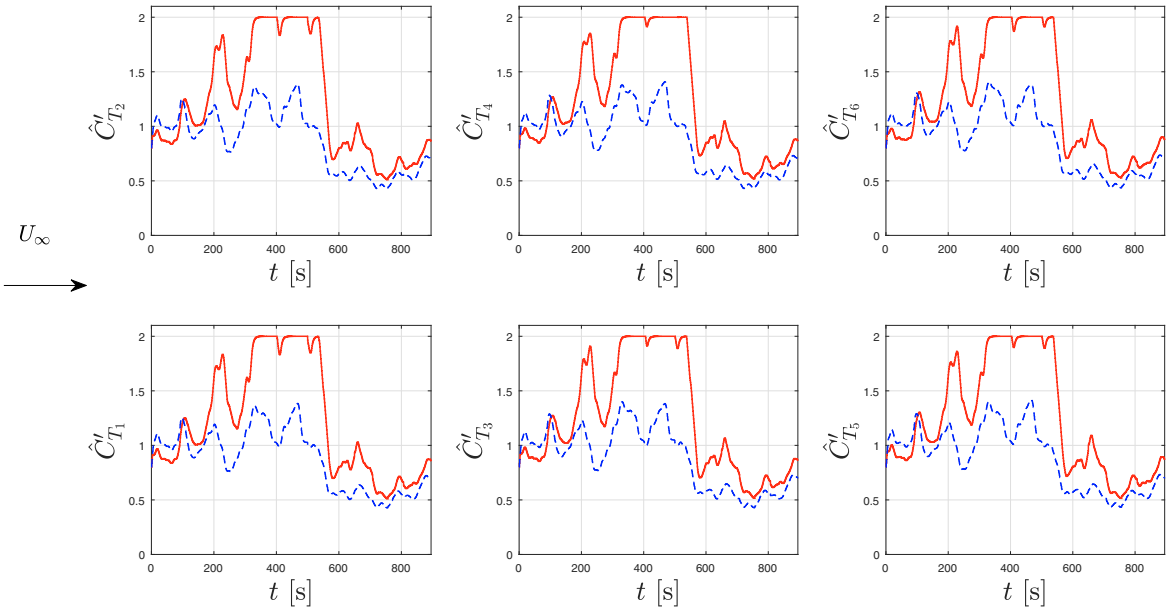

Fig. 3. Turbine control signals under $\gamma_i^* = \{-24.3, -24.3, -16.2, -16.2, 0, 0\}$ [deg] (dashed) and $\gamma_i = 0$ (solid). The black arrow on the left of the figure indicates the wind direction.

Table 1. Weight s on the variation of the force, with corresponding performance measures in percentages as given in (6).

s	⌝	$\mathrm{d}F_1$	$\mathrm{d}F_2$	$\mathrm{d}F_3$	$\mathrm{d}F_4$	$\mathrm{d}F_5$	$\mathrm{d}F_6$
50	0.94	-4.38	-1.82	-2.26	1.89	-2.43	1.82
250	-2.91	-1.95	-2.22	-0.91	-0.14	-5.94	5.28
500	1.06	-4.42	-1.86	-2.29	1.86	-2.44	1.78
1000	-2.72	-2.01	-2.28	-0.97	-0.18	-5.96	5.23

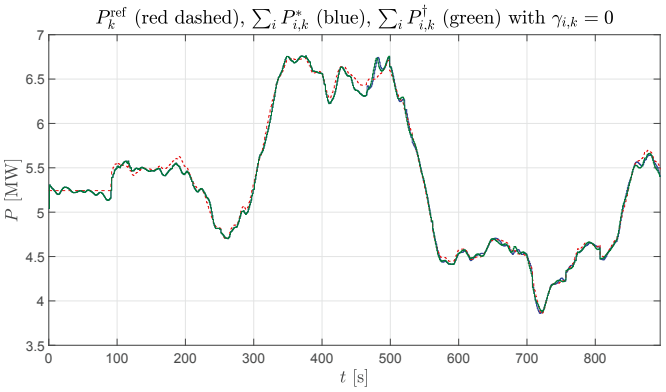

Fig. 4. Wind farm tracking results of the MPC for two different weights s. The power signal $\sum_i P_{i,k}^*$ is obtained with $s^* = 0$ and $\sum_i P_{i,k}^\dagger$ with $s^\dagger = 10^3$.

Note that here, the reference signal is not exceeding greedy power, which makes it a less challenging tracking task than presented in Section 5.2. In total, 5 simulations are performed with a different value for s in each, but under constant $q = 10^4, r = 10^4$ that are found after tuning the controller. Table 1 gives the performance measures that correspond to the different values of the weight s.

From Table 1 it can be concluded by looking at the value $\sum_i \mathrm{d}F_i$, that increasing the weight s results, on a farm level, in a decrease in the axial force variation over the complete simulation horizon. There are however local increases (see for example turbine 6), which yet need to be understood. Nevertheless, tracking is ensured in all cases (see Fig. 4) and is not significantly changing according to changes in the weight s.

5.4 Time Varying Atmospheric Conditions

In this section, simulation results are presented in which the lateral flow velocity component $\tilde{v}_k$ across the complete farm is perturbed as follows:

$$\overline{v}_k = \begin{cases} \tilde{v}_k + 0.01\tilde{v}_k, & \text{if } k > 550 \text{ and } k < 600, \\ \tilde{v}_k + 0.01\tilde{v}_k, & \text{if } k > 800 \text{ and } k < 850, \\ \tilde{v}_k, & \text{otherwise.} \end{cases} \quad (9)$$

The perturbation of $\tilde{v}_k$ is applied before time integration of the Navier-Stokes equations in PALM and yields $\overline{v}_k$. The latter is then used to compute the flow velocity components $\tilde{u}_{k+1}, \tilde{v}_{k+1}, \tilde{w}_{k+1}$. The wind farm power reference signal is given in (8) and equal controller parameters as presented before are used.

In Fig. 5, the tracking results are depicted. It can be seen that the wind farm power signal is tracking its reference even under atmospheric flow perturbations. These atmospheric changes are captured in the parameter-varying

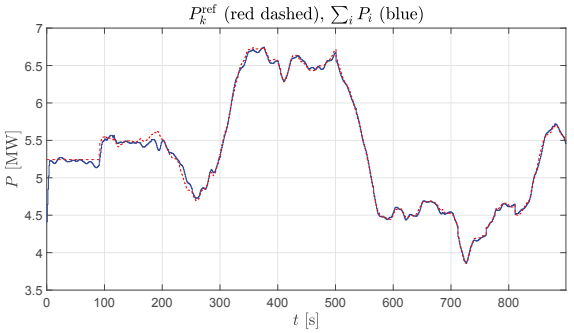

Fig. 5. Wind farm power and reference signal under atmospheric flow perturbations.

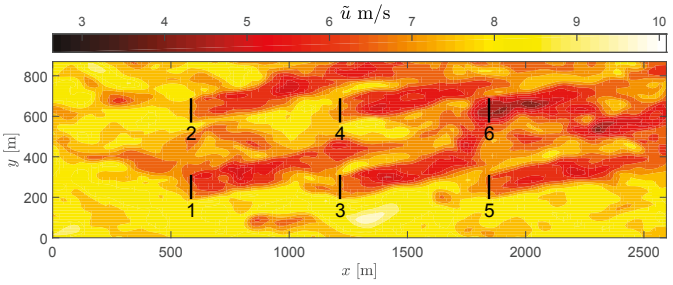

Fig. 6. Longitudinal flow field at $k = 850$ [s].

turbine models that are employed by the controller. Fig. 7, the control signals. In the latter, one can observe that the amplitude of the control signals is decreased after perturbations are applied to the lateral flow velocity component. This is due to the fact that the cross wind deflects the wakes away from the downwind rotors (see Fig. 6). As a consequence, the flow velocity components at these downwind turbines are larger, and smaller control signals are necessary to obtain the desired power.

6. CONCLUSIONS

In this paper, we formulated and implemented a constrained model predictive controller (MPC) in the high-fidelity Parallelized Large-Eddy Simulation Model (PALM). The MPC provides secondary frequency regulation and we showed that it is interesting to include, beside the thrust coefficient, also the yaw angles as control variables when tracking a reference signal above greedy power. We showed that, when properly chosen, different yaw settings can increase the available power as defined in this paper. In the MPC, the available power and wind farm power reference are considered constant during each prediction horizon. This makes our proposed closed-loop framework applicable when there is no prior knowledge on the power reference signal. On the other hand, the wind farm available power depends, i.a., on the control settings of upwind turbines. This dependency is not taken into account in the optimization, but could be included by incorporating a wake model in the MPC. Future work focusses on eliminating the imposed distribution and instead, make the MPC find a control signal distribution such that power tracking is ensured and possible other performance measures are optimized.

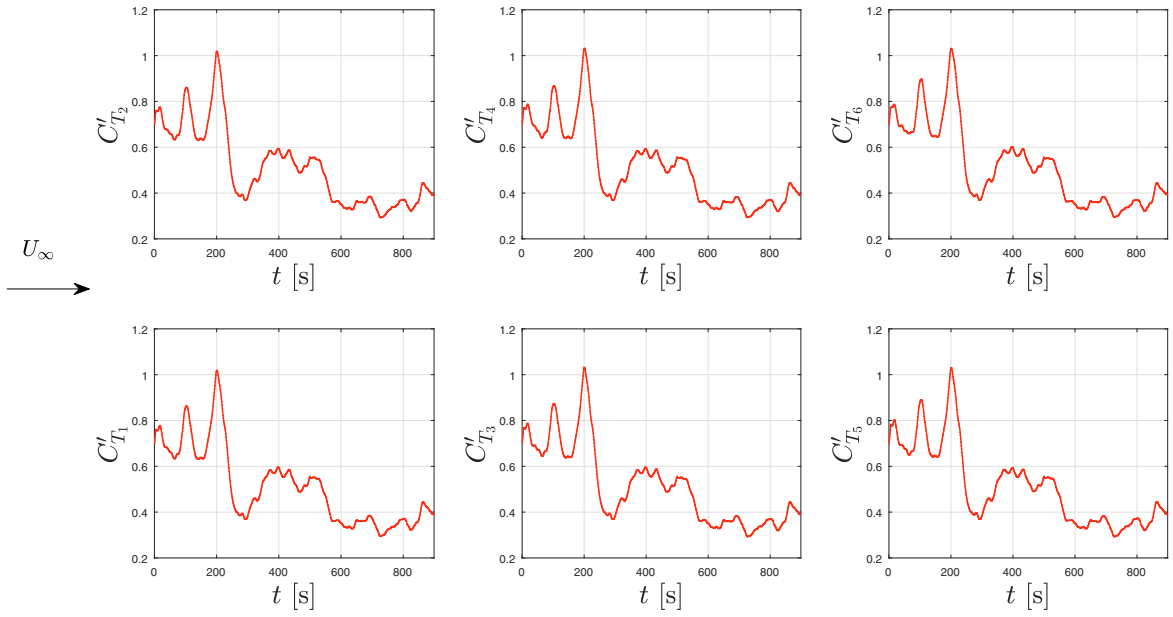

Fig. 7. Control signals under atmospheric flow perturbations. The arrow on the left indicates the wind direction.

REFERENCES

Bastankhah, M. and Porte-Agél, F. (2016). Experimental and theoretical study of wind turbine wakes in yawed conditions. *Journal of Fluid Mechanics*.

Betz, A. (1926). *Wind-Energie und ihre Ausnutzung durch Windmühlen*.

Biegel, B., D. Madjidian, D., Spudić, V., Rantzer, A., and Stoustrup, J. (2013). Distributed low-complexity controller for wind power plant in derated operation. *International Conference on Control Applications*.

Boersma, S., Doekemeijer, B.M., Gebraad, P.M.O., Fleming, P.A., Annoni, J., Scholbrock, A.K., Frederik, J.A., and van Wingerden, J.W. (2017). A tutorial on control-oriented modelling and control of wind farms. *American Control Conference*.

Boersma, S., Rostampour, V., Doekemeijer, B.M., and van Wingerden, J.W. (2018). A centralized model predictive wind farm controller in PALM providing power reference tracking. *Journal of Physics: Conference Series*.

Doekemeijer, B. (2018). github.com/TUDelft-DataDrivenControl/FLORISSE_M.

Ela, E., Gevorgian, V., Fleming, P.A., Zhang, Y.C., Singh, M., Muljadi, E., Scholbrock, A., Aho, J., Buckspan, A., Pao, L.Y., Singhvi, V., Tuohy, A., Pourbeik, P., Brooks, D., and Bhatt, N. (2014). Active power controls from wind power: Bridging the gaps. Technical report, National Renewable Energy Laboratory.

Enerdata (2017). Global Energy Statistical Yearbook. Technical report.

Fleming, P.A., Aho, J., Gebraad, P.M.O., Pao, L.Y., and Zhang, Y. (2016). Computational fluid dynamics simulation study of active power control in wind plants control in wind plants. *American Control Conference*.

Hansen, A.D., Sørensen, P., Iov, F., and Blaabjerg, F. (2006). Centralised power control of wind farm with doubly fed induction generators. *Renewable Energy*.

Madjidian, D., Mortensson, K., and Rantzer, A. (2011). A distributed power coordination scheme for fatigue load reduction in wind farms. *American Control Conference*.

Maronga, B., Gryschka, M., Heinze, R., Hoffmann, F., Kanani-Sühring, F., Keck, M., Ketelsen, K., Letzel, M.O., Sühring, M., and Raach, S. (2015). The Parallelized Large-Eddy Simulation Model (PALM) version 4.0 for atmospheric and oceanic flows: model formulation, recent developments, and future perspectives. *Geoscientific Model Development*.

Meyers, J. and Meneveau, C. (2010). Large Eddy Simulations of large wind-turbine arrays in the atmospheric boundary layer. *Aerospace Sciences Meeting*.

Pilong, C. (2013). PJM Manual 12: Balancing Operations. Technical report, PJM.

Shapiro, C.R., Bauweraerts, P., Meyers, J., Meneveau, C., and Gayme, D.F. (2017). Model-based receding horizon control of wind farms for secondary frequency regulation. *Wind Energy*.

Siniscalchi-Minna, S., Bianchi, F.D., and Ocampo-Martinez, C. (2018). Predictive control of wind farms based on lexicographic minimizers for power reserve maximization. *American Control Conference*.

Spudić, V., Jelavić, M., Baotić, M., and Perić, N. (2010). Hierarchical wind farm control for power/load optimization. *Journal of Physics: Conference Series*.

Vali, M., Petrovic, V., Steinfeld, G., Pao, L.Y., and Kühn, M. (2018). Large-eddy simulation study of wind farm active power control with a coordinated load distribution. *Journal of Physics: Conference Series*.

van Wingerden, J.W., Pao, L.Y., Aho, J., and Fleming, P.A. (2017). Active power control of waked wind farms. *International Federation of Automatic Control*.